

Prediction of flood-induced flows in urban residential areas and damage reduction

SHOJI FUKUOKA

Dept. of Civil and Environ. Engineering, Hiroshima University, Higashi Hiroshima City, Japan

MIKIO KAWASHIMA

Graduate School of Engineering, Hiroshima University, Japan

1 INTRODUCTION

Many major cities that provide the infrastructure for Japan's socioeconomic activity, lie in the floodplains of large rivers. However, the Japanese population, resources, and central administrative functions concentrate in these cities. Therefore, if embankments were to breach during a major flood, not only would the toll be high in terms of human lives and property, but also there is the danger of Japan's socioeconomic activity being thrown into a state of unimaginable confusion. Despite this situation, while the provision of flood control facilities is proceeding steadily in Japan, the current facilities are still inadequate and achieving the planned level of safety will involve considerable time and expense. Furthermore, a characteristic of natural disasters is that the possibility of flooding on a scale exceeding the design flood cannot be totally ruled out. In other words, major flooding is an ever present danger.

The Japanese socioeconomic infrastructure has already developed to the extent that a major disaster would be unacceptable, and at the very least the lives of the inhabitants must be protected and the effects of a flood disaster kept to an absolute minimum. To achieve this, it is necessary to develop flood control measures to avoid a crisis situation. In addition to structural measures, such as the provision of high specification embankments (Super Embankments), facilities for the broadcasting of flood warning and evacuation information, and the setting up of river disaster prevention stations, measures related to human activity during flooding are also being developed. Such non-structural measures include the formation of evacuation plans, the provision of information to the public by the distribution of hazard maps, on which are shown previously recorded flooded regions and predicted flooded regions, the organization of disaster relief, and the strengthening of flood fighting. In many cases, to prepare the optimum flood control plans and countermeasures, analysis of the effects of flooding is necessary, and these analyses require the prediction of floodwater behavior with a high degree of accuracy. For this reason a floodwater simulation model is required. For the prediction of the time taken for floodwaters to arrive, a prime factor in the preparation of evacuation plans, a high degree of accuracy cannot be achieved without the accurate modeling of micro-topographical features within the flooded region, such as roads, waterways, and embankments, and of

the resistance of houses and buildings. This is of particular importance in urban residential areas.

Research involving flood simulation models in the past has focused on constructing models to reproduce past flood conditions (Iwasa et al. 1980, Nakagawa 1989). However, the setting of various coefficients used has been ambiguous, and the models lack generality. The mechanism of floodwater flows in urban residential districts has been studied by Fukuoka et al. (1994, 1996), and at the Public Works Research Institute (PWRI) (Kuriki et al. 1996), using flood model experiments, and simulation models have been developed to reproduce these results; however, there still remains the problem of how to deal with groups of buildings and the network of roads in urban residential districts.

This paper describes research carried out to solve this problem. Hydraulic model experiments were carried out to investigate floodwater behavior in urban residential districts, and to study the effects of different building arrangements on the hydrodynamic forces acting on the buildings. Then, with the results of these experiments, a numerical analysis model was constructed taking buildings and the road network into consideration, and the applicability of the model was studied. Finally, a case study was made, and flood disaster prevention measures were formed from an analysis using a model to study evacuation methods. The effectiveness was analyzed and disaster prevention measures are presented.

2 HYDRAULIC MODEL EXPERIMENTS

2.1 *Large scale model experiments*

2.1.1 *Outline of the experiments*

As shown in Figures 1 and 2, water was allowed to flow through an experimental flume in which buildings and roads were arranged to model an actual urban area. Experiments were performed with two models in which the arrangement of buildings and gradient of the ground were different.

In Experiment A (Fig. 1), two types of buildings, small and large, were arranged to represent houses and apartment buildings respectively, in a region of length 5.0 m, width 2.2 m, and having a gradient of 1/2000. In the center is a trunk road around which there are small straight roads aligned in the flow direction. The scale of the model is 1/100.

In Experiment B (Fig. 2), an actual urban district was represented in which the trunk road runs diagonally and there is variation in the arrangement and density of the buildings. The region has a length of 9 m, width of 4 m, and a gradient of 1/600. The scale of the model is 1/50.

The behavior of floodwater flow in an urban district was studied by detailed measurement of flow velocities and water levels within the model.

In Experiment A, as shown in Figure 1, the spacing between buildings is only varied in the flow direction. The effects of building spacing and degree of building concentration were studied. In Case A-1, the distance between buildings is about double the building width, and the percentage of space occupied by buildings is 14%. In Case A-2, the distance between buildings is about 0.75 times the building width, and the percentage of space occupied by buildings is 25%.

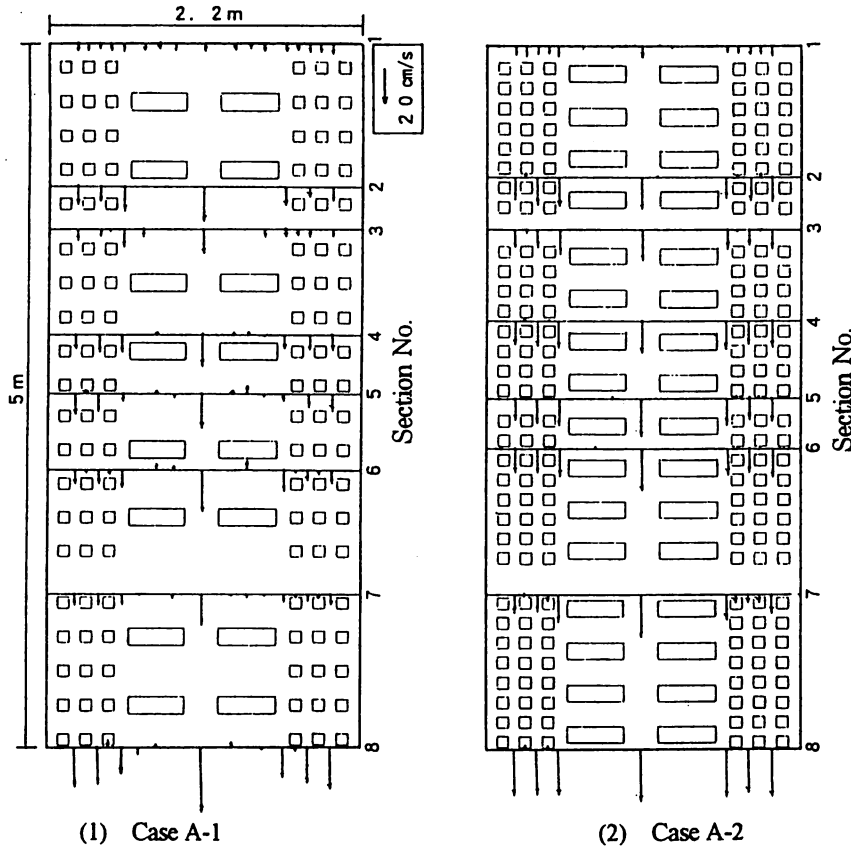


Figure 1. Flow vector diagram (Experiment A).
1. Case A-1, 2. Case A-2.

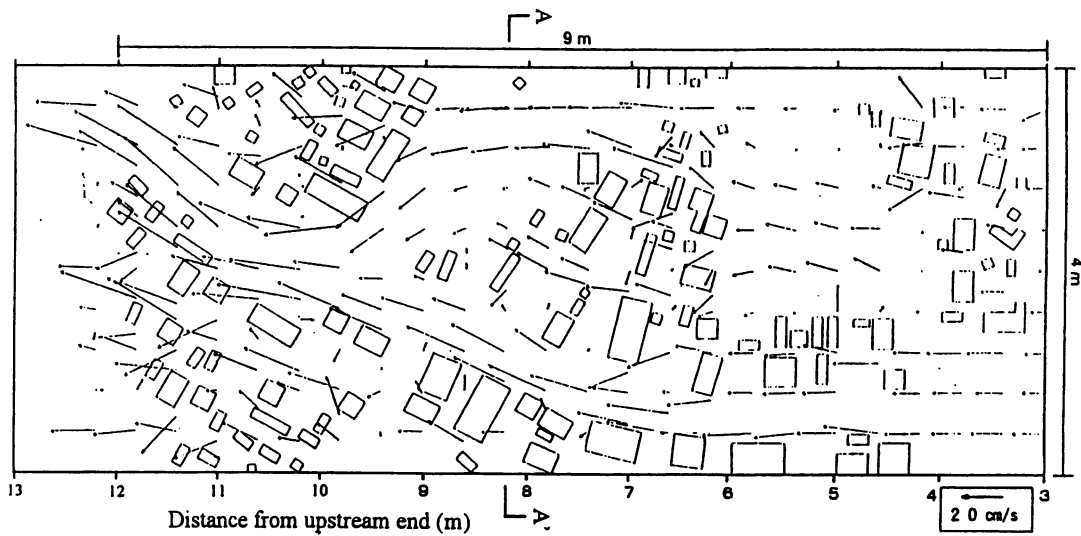


Figure 2. Flow vector diagram (Experiment B).

2.1.2 Experimental results

Characteristics of floodwater flows in urban residential districts

The vector diagrams for Experiments A and B are shown in Figures 1 and 2 respectively. It can be seen that the flow velocities over roads is high in comparison with

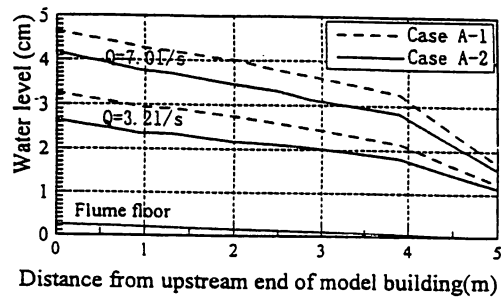


Figure 3. Water level profile (Experiment A).

the flow between buildings. This is particularly true over the wide main road. On the other hand, vortices have formed in the wake of buildings, and the flow velocity has become very slow. If this is expressed in terms of flow rate, the maximum percentage of flow over the main road in Case A-1 of Experiment A is 37% (road width is 13% of flume width), and in Case A-2 is 43% (width again 13% of flume). In Experiment B, the maximum percentage of flow over the main road is 30% (width is 10% of flume). These results indicate that the flow is concentrated over the roads.

Building resistance characteristics

Figure 3 shows the longitudinal profile of average water level of the floodwater flow for different building spacing. For all flow rates the water levels are higher for Case A-1, in which the buildings are widely spaced, compared with the levels of Case A-2, where the buildings are narrowly spaced. Generally, vortices form behind the buildings offering resistance to the flow. In the case of widely spaced buildings, there is adequate space for vortex formation and the resistance is large. On the other hand, in the case of narrowly spaced buildings, there is insufficient space for the complete formation of the vortices, and so the resistance is less.

From the results of these experiments it can be seen that the behavior of the floodwater flow in urban residential districts is greatly influenced by the arrangement of the buildings and roads (Fukuoka et al. 1994), and that the accuracy of the predictions obtained from the model is determined by how well this arrangement is incorporated.

2.2 *Hydrodynamic forces acting on buildings*

2.2.1 *Outline of the experiments*

The main factors in the resistance to the floodwater flow are: the resistance of the ground surface, the resistance due to the plane vortices formed between the slow flow behind buildings and the more rapid flow between the buildings, and the hydrodynamic forces (lift and drag) resulting from the flow around the building. For the purpose of modeling these hydrodynamic forces, experiments were performed to directly measure the forces acting on the buildings.

As was indicated by the large scale model experiments, the arrangement of the buildings influences the flow through an urban residential district which in turn affects the hydrodynamic forces. The flow and the hydrodynamic force characteristics were studied with various building arrangements and spacing.

An experimental flume of length 2.7 m, width 1.35 m, and having a gradient of about 1/700 was used. Model buildings 15 cm square were arranged in the flume,

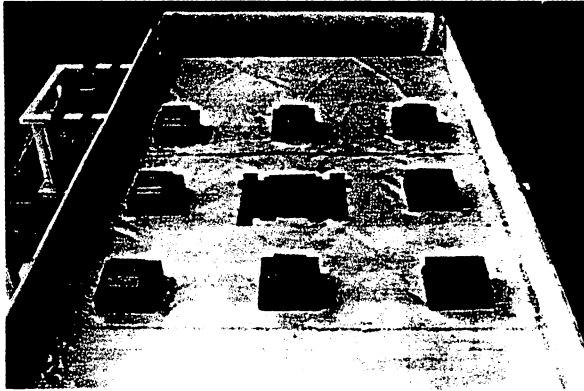


Figure 4. Model for measuring hydrodynamic forces.

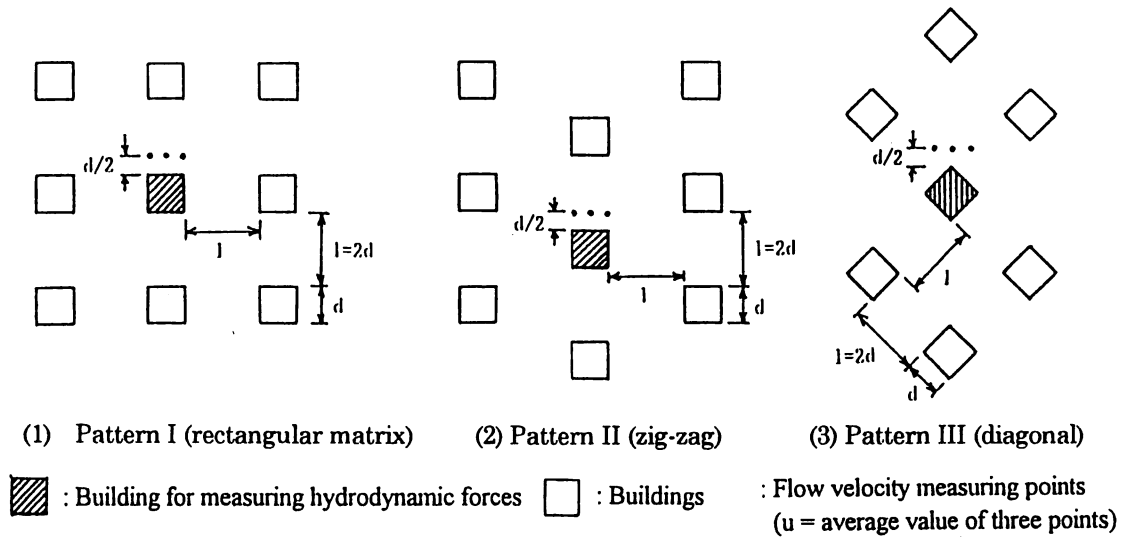


Figure 5. Building arrangement patterns. 1. Pattern I (rectangular matrix), 2. Pattern II (zig-zag), 3. Pattern III (diagonal).

force component gauges were attached to the building in the center region, and drag and lift forces were measured directly in the flow direction and lateral direction. The overview of hydrodynamic force measuring experiments can be seen in Figure 4.

To study the differences in hydrodynamic forces due to differing building arrangements, the experiments were conducted using the arrangements shown in Figure 5. In Pattern I the buildings were arranged in a rectangular 3×3 matrix, in Pattern II a zig-zag arrangement was adopted, and Pattern III represents the case where the floodwater flows diagonally. The distance between buildings was set at twice the width in each case and a comparison was made. The distance between buildings was changed in the flow direction for Pattern I to determine the effects on the hydrodynamic forces.

The flow velocity used was the average of the velocities measured at three points located in a section lateral to the flow direction, a distance of one half building width upstream, as shown in Figure 5. This location was chosen because of the build-up of

water in the vicinity of the building and the fact that reverse flow is small at a distance of 1/2 the building width or more upstream.

2.2.2 Experimental results

In Table 1 are shown the values of drag D ($\rho C_D u^2 A/2$), lift L ($\rho C_L u^2 A/2$), and the coefficient of drag C_D . The values of drag for Pattern I (rectangular matrix) and for Pattern II (zig-zag) were small, and there was little difference between them. In the case of Pattern III (diagonal), however, a large drag force was indicated. This is because in the case of Patterns I and II the flow concentrates in the roads and flows downstream, whereas in the case of Pattern III, the concentrated flow directly hits the buildings. However, if the average flow velocity u on the front surface of the building (the average of the three points shown in Fig. 5), is used to calculate the coefficient of drag, there is no significant difference in the values, values of about $C_D = 3$ were obtained for all patterns. This shows that while there is a large difference in the drag force caused by the different flows for the various patterns, the coefficient of drag can be represented by a constant. It was also found that the lift was small, being about 15% to 30% of the drag.

In Figure 6 is shown the relationship between building spacing/building width (l/d) and drag and drag coefficient. When $l/d \leq 3$, the drag force is extremely small but rises rapidly for $l/d > 3$. This is because at $l/d \leq 3$, the building is in the wake of the building in front and the flow velocity is small. Considering the coefficient of drag, for $l/d \geq 4$ $C_D = 5$, a value roughly corresponding to the drag coefficient of an isolated building. From this it can be seen that there is a close relationship between the drag coefficient and building spacing.

Table 1. Results of the hydrodynamic force measuring experiment (Relationship with building arrangement pattern).

Pattern	Drag D (gf)	Lift L (gf)	Drag coefficient (C_D)
I	5.9	1.9	2.8
II	4.1	0.8	3.5
III	50.9	7.6	3.7
Isolated building	41.6	3.4	4.5

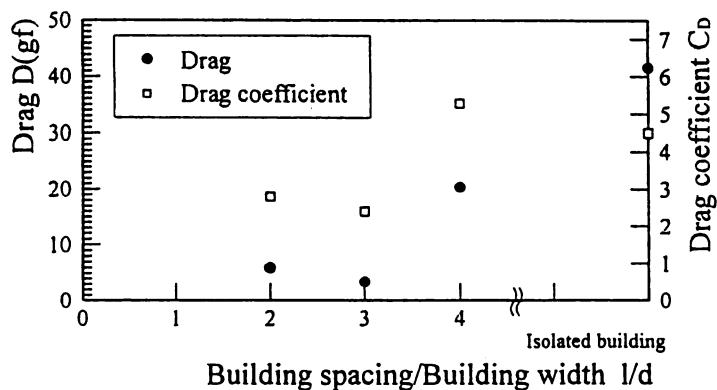


Figure 6. Variation of drag and drag coefficients with ratio of building spacing and building width.

3 NUMERICAL ANALYSIS OF THE FLOODWATER FLOW

Generally, a two dimensional shallow water model can be applied to represent a flood flow spreading in a large floodplain. Particularly in cases where highly accurate information is required for such things as floodwater propagation characteristics it is necessary to use a precise two dimensional unsteady flow model (Kuriki et al. 1996). However, previously used two dimensional unsteady flow models used a calculation grid having typical dimensions from several hundreds of meters up to one kilometer. The incorporation of detailed topography such as roads, that affect the behavior of floodwater flow in urban districts, into such models was impossible. Also, the buildings within the urban district become a resistance factor that varies with the density and arrangement of the buildings. Until now, practical models were mainly achieved by applying a roughness coefficient equivalent to the building density for different categories of land replacing the resistance of groups of buildings with surface friction. As the resistance is not expressed generally, there were problems resulting from unsuitable representation (Fukuoka et al. 1994). Recently, the Public Works Research Institute (Kuriki et al. 1996) have proposed a method of calculating an equivalent roughness coefficient that is a function of the building density ratio, surface roughness coefficient, and floodwater depth. However, this still does not overcome the problems arising due to replacing resistance of groups of building with surface friction.

The flood simulation model (Fukuoka et al. 1996) used for the research described in this paper employs the general curvilinear coordinate system shown in Figure 7, in which the axes can be set on any curve. This enables the road network to be reproduced accurately and at the same time, by choosing the calculating grid size for groups of buildings. Since groups of buildings are represented as impermeable obstructions to the flow, the hydrodynamic forces on the buildings can be incorporated in the basic equations.

3.1 Calculation method

3.1.1 Basic equations

The basic equations are the shallow water flow equations expressed in the general curvilinear coordinate system.

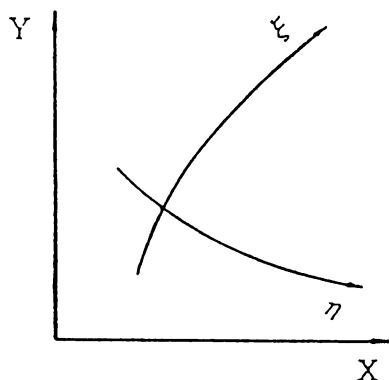


Figure 7. Rectangular coordinate system and general curvilinear coordinate system.

Continuity equation:

$$\frac{\partial h}{\partial t} \frac{1}{J} + \frac{\partial u^\xi h}{\partial \xi} \frac{1}{J} + \frac{\partial u^\eta h}{\partial \eta} \frac{1}{J} = 0 \quad (1)$$

and the equation of motion in the ξ direction will be given by:

$$\begin{aligned} & \frac{\partial u^\xi h}{\partial t} \frac{1}{J^2} + \frac{\partial (u^\xi)^2 h}{\partial \xi} \frac{1}{J^2} + \frac{\partial u^\xi u^\eta h}{\partial \eta} \frac{1}{J^2} - \frac{h}{J} u^x \left(u^\xi \frac{\partial \xi_x}{\partial \xi} \frac{1}{J} + u^\eta \frac{\partial \xi_x}{\partial \eta} \frac{1}{J} \right) \\ & - \frac{h}{J} u^y \left(u^\xi \frac{\partial \xi_y}{\partial \xi} \frac{1}{J} + u^\eta \frac{\partial \xi_y}{\partial \eta} \frac{1}{J} \right) + \frac{gh}{J} \left(\alpha \frac{\partial H}{\partial \xi} + \beta \frac{\partial H}{\partial \eta} \right) + \frac{gn^2 u^\xi}{J^2 h^{1/3}} \\ & \left\{ (u^x)^2 + (u^y)^2 \right\}^{1/2} - \frac{\varepsilon}{J} \left\{ \begin{aligned} & \xi_x \left(\alpha \frac{\partial^2 u^x h}{\partial \xi^2} + 2\beta \frac{\partial^2 u^x h}{\partial \xi \partial \eta} + \gamma \frac{\partial^2 u^x h}{\partial \eta^2} \right) + \\ & \xi_y \left(\alpha \frac{\partial^2 u^y h}{\partial \xi^2} + 2\beta \frac{\partial^2 u^y h}{\partial \xi \partial \eta} + \gamma \frac{\partial^2 u^y h}{\partial \eta^2} \right) \end{aligned} \right\} \\ & - \frac{1}{J^2} (\xi_x F_x + \xi_y F_y) = 0 \end{aligned} \quad (2)$$

and the equation of motion in the η direction will be given by:

$$\begin{aligned} & \frac{\partial u^\eta h}{\partial t} \frac{1}{J^2} + \frac{\partial u^\xi u^\eta h}{\partial \xi} \frac{1}{J^2} + \frac{\partial (u^\eta)^2 h}{\partial \eta} \frac{1}{J^2} - \frac{h}{J} u^x \left(u^\xi \frac{\partial \eta_x}{\partial \xi} \frac{1}{J} + u^\eta \frac{\partial \eta_x}{\partial \eta} \frac{1}{J} \right) - \\ & \frac{h}{J} u^y \left(u^\xi \frac{\partial \eta_y}{\partial \xi} \frac{1}{J} + u^\eta \frac{\partial \eta_y}{\partial \eta} \frac{1}{J} \right) + \frac{gh}{J} \left(\beta \frac{\partial H}{\partial \xi} + \gamma \frac{\partial H}{\partial \eta} \right) + \frac{gn^2 u^\eta}{J^2 h^{1/3}} \\ & \left\{ (u^x)^2 + (u^y)^2 \right\}^{1/2} - \frac{\varepsilon}{J} \left\{ \begin{aligned} & \eta_x \left(\alpha \frac{\partial^2 u^x h}{\partial \xi^2} + 2\beta \frac{\partial^2 u^x h}{\partial \xi \partial \eta} + \gamma \frac{\partial^2 u^x h}{\partial \eta^2} \right) + \\ & \eta_y \left(\alpha \frac{\partial^2 u^y h}{\partial \xi^2} + 2\beta \frac{\partial^2 u^y h}{\partial \xi \partial \eta} + \gamma \frac{\partial^2 u^y h}{\partial \eta^2} \right) \end{aligned} \right\} - \\ & \frac{1}{J^2} (\eta_x F_x + \eta_y F_y) = 0 \end{aligned} \quad (3)$$

where h = water depth, H = water level ($= h + z$, z : ground elevation), u^ξ = flow velocity in the ξ direction, u^η = flow velocity in the η direction, ε = eddy viscosity coefficient of flow

$$\varepsilon = \frac{\kappa}{6} u_* h \quad (4)$$

where κ = Karman constant (0.4), u_* = friction velocity ($= \sqrt{\tau/\rho}$), τ = bed shear stress, ρ = water density, $\xi_x = \partial \xi / \partial x$, $\xi_y = \partial \xi / \partial y$, $\eta_x = \partial \eta / \partial x$, $\eta_y = \partial \eta / \partial y$, J = Jacobian operator ($= \xi_x \eta_y - \xi_y \eta_x$), u^x = the flow velocity in the x direction ($= (1/J)(\eta_y u^\xi - \xi_y u^\eta)$),

u^y = the flow velocity in the y direction ($= (1/J)(\xi_x u^\eta - \eta_x u^\xi)$), $\alpha = (1/J)(\xi_x^2 + \xi_y^2)$, $\beta = (1/J)(\xi_x \eta_x + \xi_y \eta_y)$, $\gamma = (1/J)(\eta_x^2 + \eta_y^2)$, F_x = the component of hydrodynamic force F in the x direction, F_y = the component of hydrodynamic force F in the y direction,

$$F_x = -\frac{1}{2} \left(C_D u^x + C_L u^y \frac{\Delta U}{|\Delta U|} \right) \sqrt{\{(u^x)^2 + (u^y)^2\}} \frac{A}{A'} \quad (5)$$

$$F_y = -\frac{1}{2} \left(C_D u^y + C_L u^x \frac{\Delta U}{|\Delta U|} \right) \sqrt{\{(u^x)^2 + (u^y)^2\}} \frac{A}{A'} \quad (6)$$

where A = the projected area of a building in the main flow direction, A' = area of calculation grid on which hydrodynamic forces act, C_D = coefficient of drag, C_L = coefficient of lift, U = flow velocity in the main flow direction ($= \sqrt{\{u^x\}^2 + \{u^y\}^2}$), ΔU = flow velocity difference between two planes parallel to the main flow direction ($\Delta U = U_2 - U_1$).

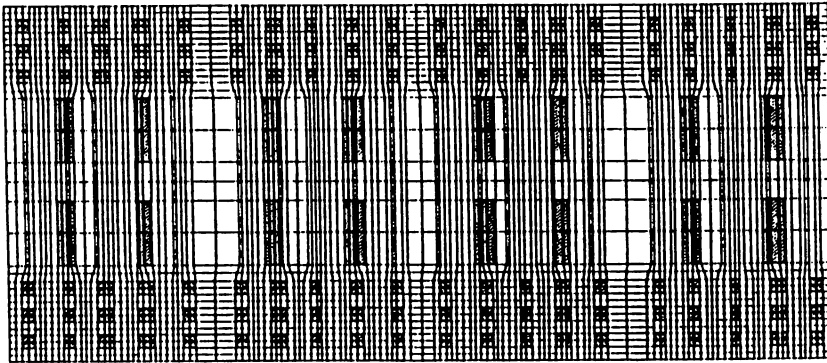


Figure 8. Floodwater flow numerical analysis grid model (Experiment A).

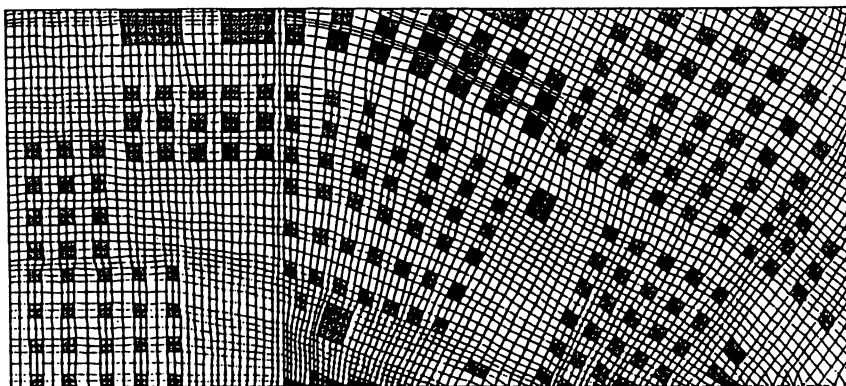



Figure 9. Floodwater flow numerical analysis grid model (Experiment B).

3.1.2 Modeling of the floodplain

Figures 8 and 9 are the numerical analysis grid models for the hydraulic models used for Experiments A and B respectively. The grid was divided to conform to the roads and residential regions, and the buildings are modeled by the grid (shown by the symbol  in the Figs 8 and 9). The height of the building grid was made the same as the actual building and impervious to the flow. In the model for Experiment B, the actual building arrangement was modeled by simplifying into a regular arrangement as shown in Figure 9. The building density ratio was the same as for the actual case.

The value of coefficient of drag was taken from the relationship shown in Figure 10 that was obtained as a result of the hydrodynamic force measuring experiments and is independent of the building arrangement. The coefficient of lift was calculated from the value $C_L/C_D = 0.2$ obtained experimentally.

3.2 Verification of the simulation model

Figure 11 shows a comparison of the calculated and experimental results for the longitudinal profile of average water level for Experiment A. As the eddy viscosity ϵ is affected by the flow field caused by the building and road arrangement, this was included among the parameters for the simulation calculation. As a result, by taking the value as 50 times that given by Equation (4) in Case A-1 where the spacing between buildings was wide, and taking the value to be 10 times for Case A-2, good agreement was achieved with the experimental values. As can be seen from Figure 12, the cross sectional flow velocity distribution calculated using these values provided an accurate simulation.

Figure 13 shows a comparison of the calculated and experimental results for the longitudinal profile of average water level for Experiment B, and in Figure 14 is shown a comparison of the cross sectional flow velocity distribution. The value of $10 \times \epsilon$, obtained in Case A-2, where the distance between the buildings was close to the building width, was taken for the eddy viscosity. Although there are some localized areas where the simulation of the water surface contour is poor, overall the calculated water level provided a good simulation of the experimental results. The cross sectional flow velocities were close to the experimental values. These results provided a verification of the applicability of the proposed flood simulation model.

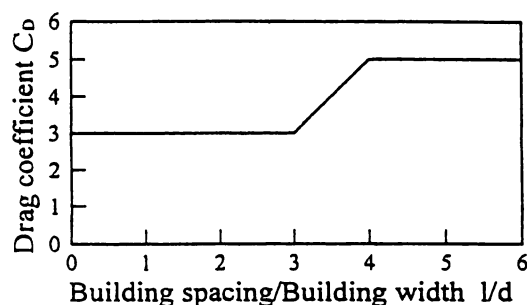


Figure 10. Drag coefficient model.

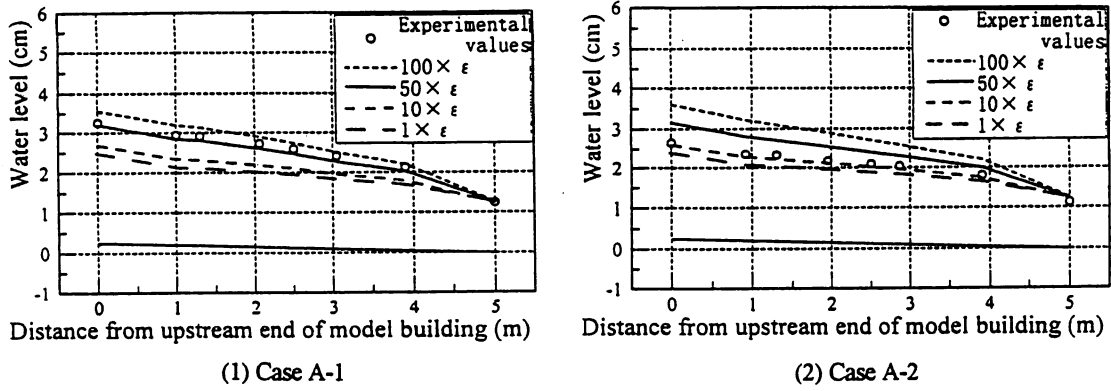


Figure 11. Comparison of experimental and calculated water levels. 1. Case A-1, 2. Case A-2.

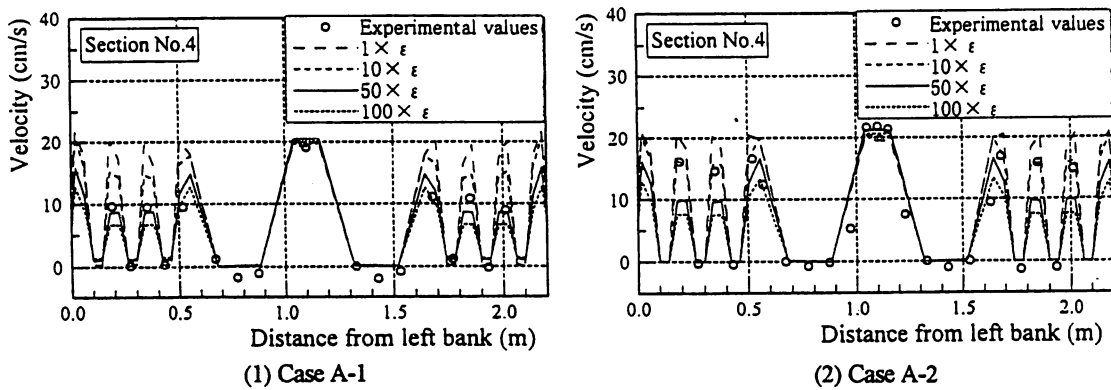


Figure 12. Comparison of calculated and experimental results for the flow velocity distribution. 1. Case A-1, 2. Case A-2.

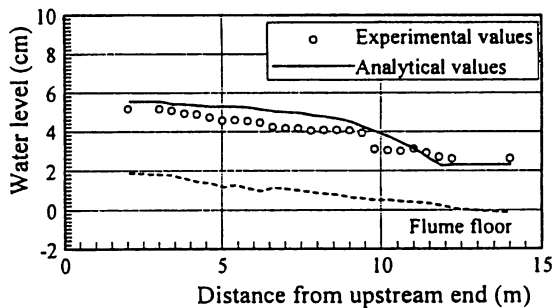


Figure 13. Comparison of the calculated and experimental results for the longitudinal profile of water level.

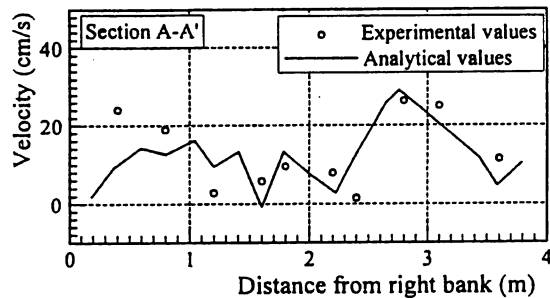


Figure 14. Comparison of the calculated and experimental lateral velocity distribution.

4 CASE STUDY OF FLOOD DISASTER PREVENTION MEASURES

Flood disaster prevention measures can be divided into two main types, the structural type measures, and the non-structural type of measures. Some of the structural type measures are the provision of Super Embankments, linear embankment structures,

waterways, and pumps etc., for flood control and floodwater drainage, and measures to maintain vital lifelines in the event of flooding, such as the provision of disaster information systems and river disaster prevention stations. Some examples of the non-structural measures are the preparation of regional disaster prevention plans such as evacuation plans, the distribution of information such as flood hazard maps, improvement of flood control activities, the organization of disaster relief, and the strengthening of flood fighting.

Of these various measures, this paper describes a case study made of the flood control and floodwater drainage, and of the evacuation plans of an actual floodplain region and discusses the concepts and the effectiveness of such measures.

4.1 *Method of study*

4.1.1 *Outline of the floodplain*

The area taken for the case study was a low-level flatland area in the Kanto region in which are situated M City and Y City. The long shaped region, shown in Figure 15, has a gradient of about 1/4000 and measures about 17 km in the north-south direction, and about 5 km in the east-west direction. The region is bounded by two major rivers, one in the west and other in the east, to form a closed region of land. Within this region there are railway lines and an expressway, the embankment structures of which have a major effect on floodwater flow, as well as a waterway network and a diversion channel. There is a pumping station situated at the end of the diversion channel. The city chosen for the study was M City, located upstream of which is Y City. The urban districts have mainly developed along the E River and the N River, and in particular, the regions north of the expressway and railway lines are highly developed urban districts.

4.1.2 *Calculation conditions*

The case where the E River in the east breached its embankment was considered for the study. The length of the breach in the embankment was calculated using Equation (7), with reference to research carried out at the Public Works Research Institute (Kuriki et al. 1996). The scale of the flood considered was the design flood for E River.

$$L_B = 1.6 \times (\text{Log}_{10} B)^{3.6} + 62 \quad (7)$$

where L_B = length of the breach (m), B = width of the river (m).

4.2 *Flood control and floodwater drainage*

4.2.1 *The case studied*

Firstly, the existing embankments, waterways, and pumping station facilities, and the flood control and floodwater drainage measures will be considered. There are a number of embankments and waterways within the region. Prevention of the floodwater dispersion by the linear embankments, early stage drainage by the waterways and pumping station, and a resulting reduction in floodwater levels can be expected. The point of the breach was taken to be the upstream end of M City where it was pre-

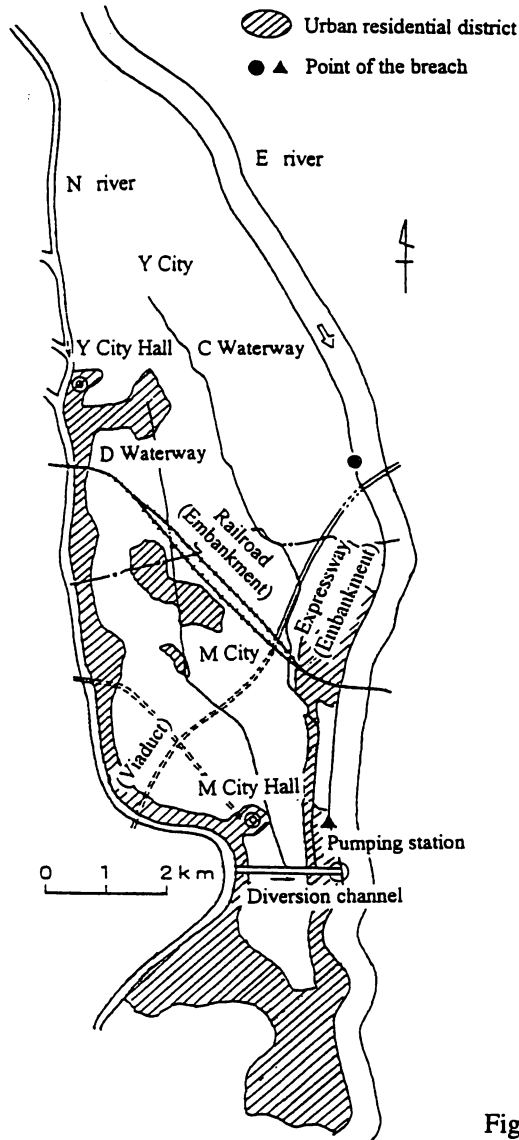


Figure 15. Case study floodplain.

dicted that the effects on the urban district would be considerable (indicated by the symbol • in Fig. 15). The cases considered were as follows:

Case 1

Water is led by pumping into the waterway network and diversion channel where it drains away. The diversion channel pumping station is designed to drain floodwaters from the flooding N River into the E River; however, there is a time difference of discharge hydrograph in E River and N River during a flood. As the discharge rate of E River is relatively slower, emergency use of the diversion channel pumping station can be considered in the event of E River breaching its embankment. The floodwaters would be led through the waterways to the pumping station.

Case 2

In this case a breach was considered upstream of M City in which the railway and

expressway embankments prevent the floodwaters from inundating the urban residential district in the center of M City. At the same time the floodwaters are led downstream via the waterway network and drained by pumping. In such a case, emergency shut-off facilities such as stoplogs would be required at the numerous embankment culverts. It would also be necessary to change the underpass portion of the waterways from open channel type to siphon type to provide a structure enabling shut-off.

4.2.2 *Analysis of the proposed measures*

In Figure 16 is shown the variation of the floodwater area with elapsed time, and Figure 17 shows the maximum inundation depth distribution. The floodwater flow would be temporarily stopped by the railway and expressway embankments, but would then proceed downstream via box culverts and the waterways where it would build up at the diversion channel embankment. The floodwater level would then rise and the water would flow back into the river over the low embankment of the N River. Also, the floodwater collected in the waterway system would be pumped out or drained naturally from the end of the diversion channel into the E River. Natural drainage would start about 40 hours after breaching of the embankment, the floodwater area would diminish rapidly. And then floodwater drainage via the waterway network becomes effective.

In Case 1, as indicated in Figure 16, the variation in floodwater area would be almost the same as for the case of no countermeasures; however, the drainage due to pumping before natural drainage starts would result in an over all reduction in the depth of the floodwater. The region covered by floodwater exceeding a depth of 1 m would be reduced by about 1 km², and the region of less than 1 m would be increased by the same amount. The maximum floodwater depth, shown in Figure 17, also indicates that the region of deep floodwater is reduced, and that the operation of the existing facilities provides an effective countermeasure. In this case, the floodwater flow rate is high, and as the pumping flow rate is small in comparison, the reduction in floodwater area and depth are not so appreciable; however, a more significant result could be expected if the scale of the flood or of the river were smaller.

In Case 2, as the increase of floodwater flow downstream was shut off, the floodwater region is confined upstream. As a result, the floodwater area becomes about 9 km², and inundation of the urban district downstream is prevented. On the other hand, the depth and size of the floodwater region upstream are increased, as is the flood duration. This is because the waterways and pumping station are inadequate to cope with the scale of the floodwater inflow. While the countermeasures are effective in reducing the overall flood damage, an upstream/downstream flow problem is caused as the result of the increased floodwater damage upstream caused in order to reduce the damage downstream. Therefore, these measures should be considered in combination with the provision of flood control facilities adequate to achieve the necessary drainage to match the scale of the upstream flooding, such as the installation of sluice pipes to enable draining downstream.

From the above it was found that the flood control and floodwater drainage measures were effective in reducing flood damage. To improve the effectiveness of these measures and provide adequate disaster control, it is necessary to provide facilities in addition to those already existing to match the scale of possible flooding.

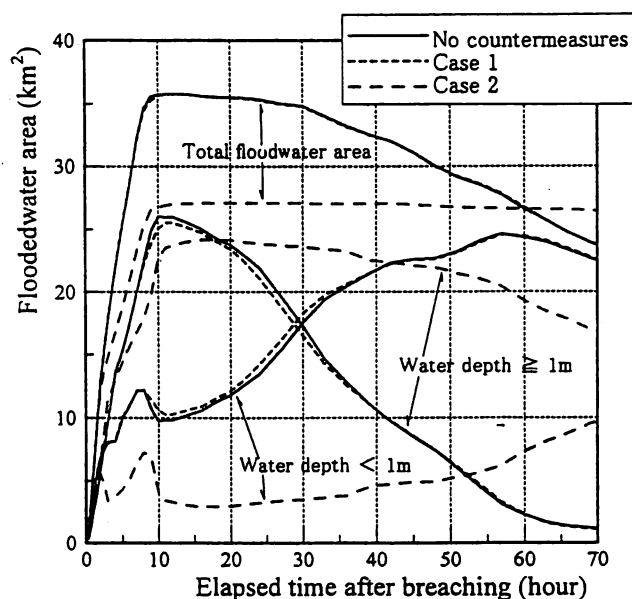


Figure 16. Variation of floodwater area and depth with time.

4.3 Study of evacuation methods

Local self-governing bodies formulate evacuation plans as part of regional disaster plans, but for the most part these plans are with respect to earthquakes, and there are many problems involved in applying such plans in the event of flooding. Even when flood disasters are considered, there are very few cases where these plans are formulated based on predicted flooding conditions. It is of major importance to formulate evacuation plans based on the dynamic flood conditions that would result from a breach in the river embankment.

For the purpose of this case study, the evacuation method and evacuation sites were considered for the center region of M City (point ▲) under the present floodplain conditions, in the event of a flood calculated for the case of an embankment breach.

Figure 18 shows the maximum floodwater depth distribution, and Figure 19 a contour map for the floodwater arrival time. The floodwater spread to cover almost the entire region enclosed within the railway and the diversion channel, and many areas had a floodwater depth of between 1 m ~ 2 m. From the flood water arrival time contour map it can be seen that the floodwater flow was particularly rapid in the first 30 minutes after breaching of the embankment. The floodwater spreads rapidly along the waterway and at the low land along the waterway.

The evacuation site must be a structure capable of withstanding the floodwater and have floors at a height greater than the maximum floodwater depth. It must also be available to, and well known by the public. For these reasons, the high level concrete school building shown in Figure 19 was chosen as the designated evacuation site. From the maximum floodwater depth distribution, any evacuation site could become flooded, so it is necessary to investigate in advance how many floors are likely to be usable by comparing the maximum floodwater depth with the height of the floors. It is also necessary to store emergency provisions that can be used on those floors.

Even if an evacuation site is designated, if it is in the vicinity of the breach in the embankment the floodwater will arrive quickly and there is the possibility that it will

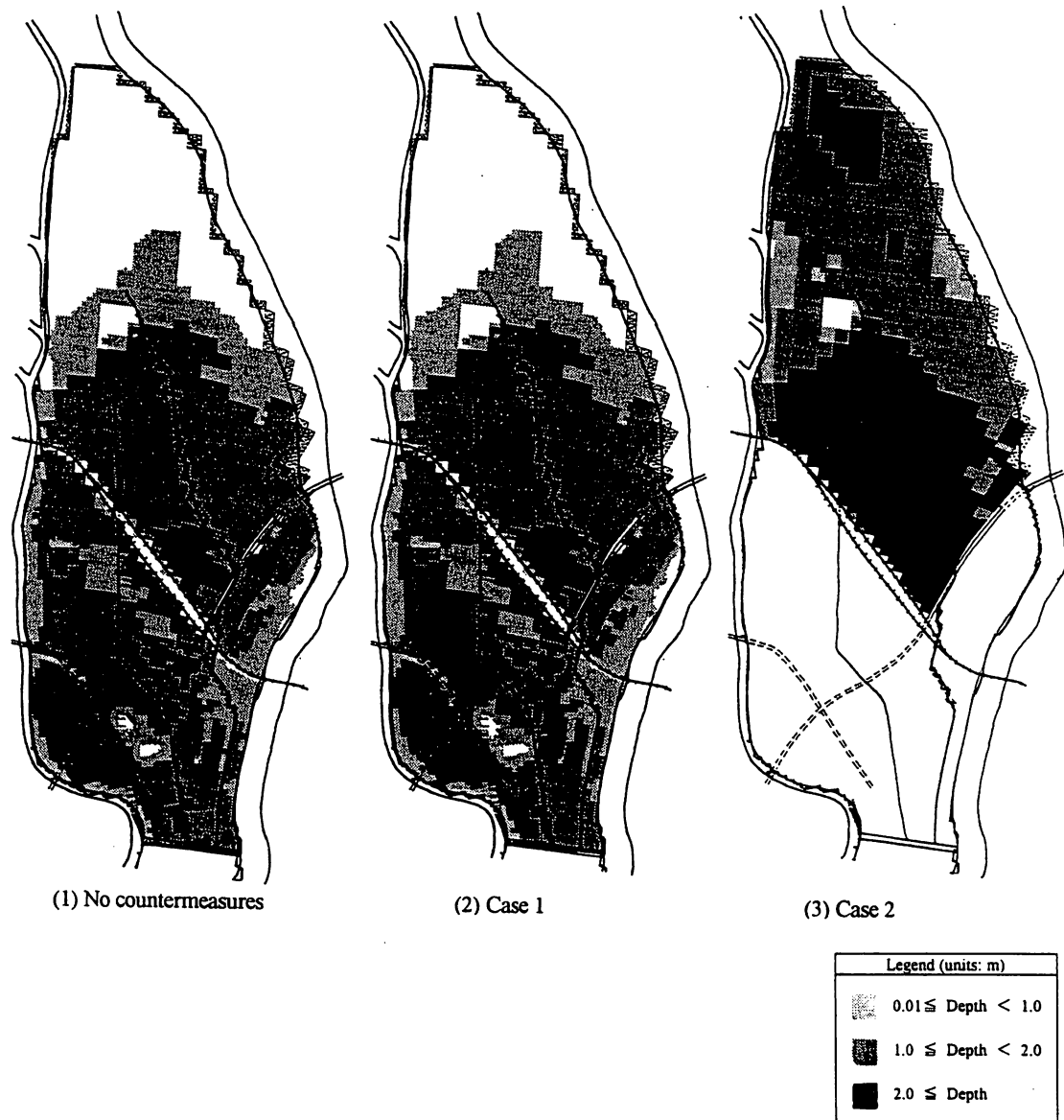


Figure 17. Maximum floodwater depth distribution. 1. No countermeasures, 2. Case 1, 3. Case 2.

become inaccessible. A method of determining the areas where such difficulties might occur is being proposed by Nishihara (1983) and Takasao et al. (1995). Their simulation models involve human behavior for evacuation. Here, in order to make a simple evaluation, it was assumed that evacuation would commence when the breach in the embankment occurs, and that inhabitants living in the region within which they could reach the site before the floodwater arrived were able to evacuate. For example, if it would take the floodwater 30 minutes to arrive at the evacuation site, then anywhere within 30 minutes walking distance of the site would be in the evacuation region for that site. For the speed of evacuation, reference was made to previous floods (Suetsugi 1995) and the case of an adult walking speed of 1.5 km/h, as well as the case of inhabitants who would have more trouble travelling, such as older people

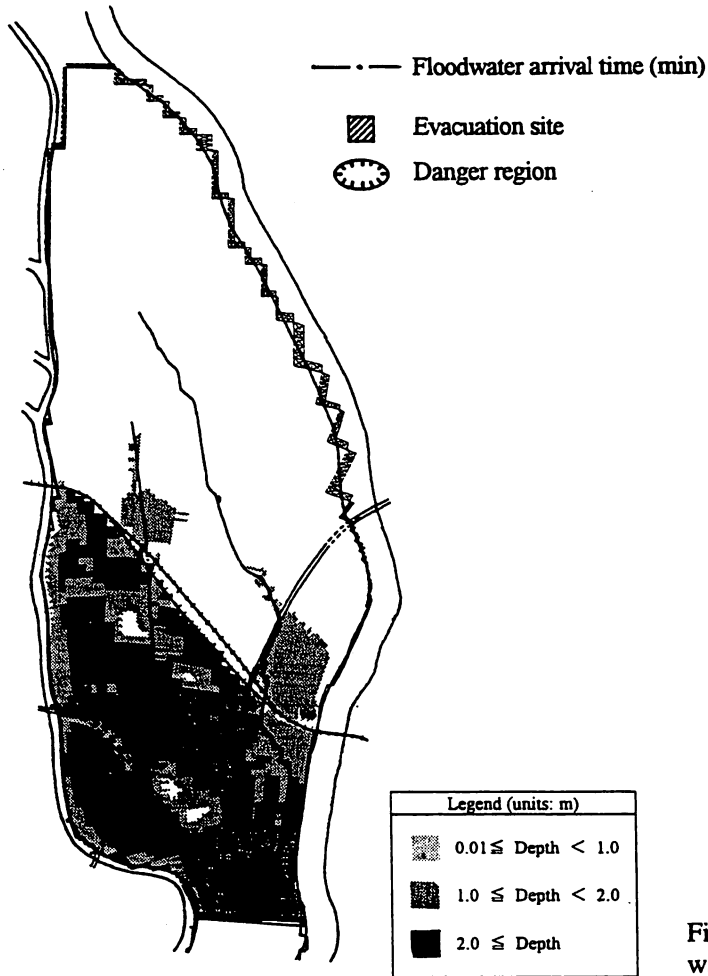


Figure 18. Distribution of maximum water depth.

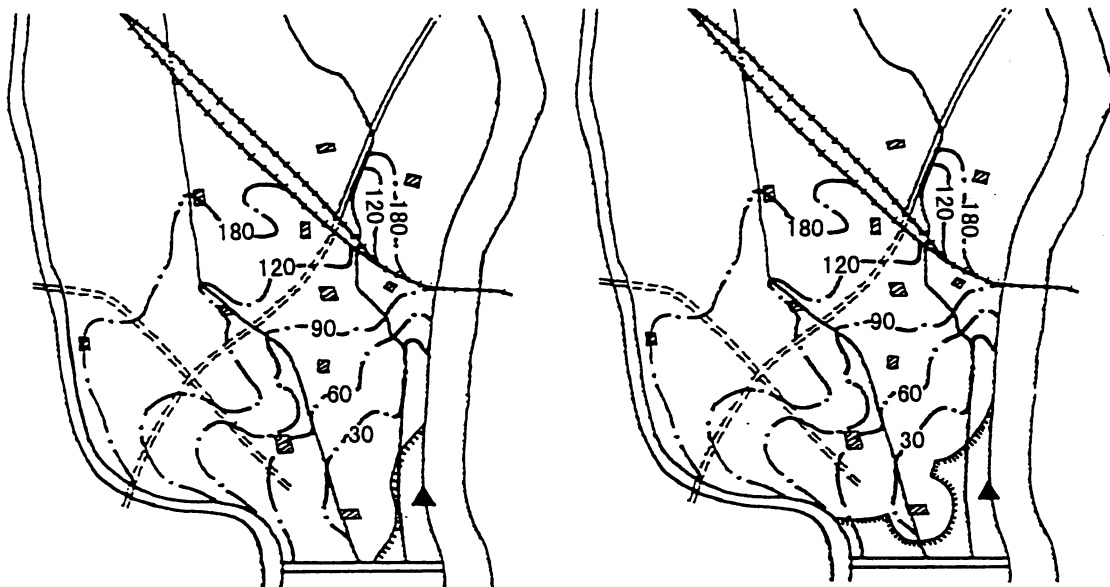


Figure 19. Floodwater arrival time contour map. 1. The case for adult walking pace, 2. The case for old people and young people.

or young children, and who were assumed to move at a speed of 1 km/h, were studied. The regions near the breach in the embankment shown in Figure 18, are areas where, in the event of a breach at the point marked ▲, would have difficulty reaching any evacuation site. Considering the case of older people and young children, it can be foreseen that the areas in which trouble in evacuating is likely would be extensive. Designating private high-rise concrete apartment buildings as evacuation sites in these areas could be considered. It is also necessary to consider the need to evacuate such danger zones in advance of actual embankment failure and provide the necessary advance warning.

In M City there are no public road constructed on embankments or viaducts. For this reason there would be no roads that could be walked safely after flooding had taken place and it would therefore be almost impossible for those who did not escape in time to evacuate. It is therefore necessary to consider in advance the use of railroads and expressways as emergency evacuation routes, temporary evacuation sites, and relief and rescue routes.

It still remains necessary to carry out the same investigation for cases where breaching of the embankment occurs at many points along E River before presenting a comprehensive evacuation plan.

CONCLUSIONS

A flood simulation model was made for an urban residential area that suitably incorporated micro-topographical features such as the network of roads, as well as the shape, arrangement, and resistance characteristics of groups of buildings. The applicability of the model was verified by reproducing the results obtained from large scale hydraulic model experiments.

The model was then used to carry out case studies of actual urban districts and flood disaster prevention measures were investigated. The case studies were carried out on the premise that the current flood control facilities would be used; however, it was found that, to effectively prevent a flood disaster, additional facilities would have to be constructed and substantial evacuation planning would be necessary.

Finally, it is important to carry out flood countermeasures to provide an integrated river and floodplain environment in which urban areas are safe from the threat of flooding.

In order to achieve this, plans must be formulated after comprehensive investigations have been made based on highly accurate flood predictions. The flood simulation model described here provides an effective means of making such predictions.

REFERENCES

- Fukuoka, S., Kawashima, M., Matsunaga, N. & Maeuchi H. 1994. Flooding Water over a Crowded Urban District. *Journal of Hydraulic, Coastal and Environmental Engineering, Japan Society of Civil Engineers* 491(II-27): 51-60.
- Fukuoka, S., Kawashima, M. & Yokoyama, H. 1996. Experiment and Analysis of Floodwater Flow in Urban Districts. *Proceedings of the Annual Meeting of the Chugoku Branch of the Japan Society of Civil Engineers*: 217-218.

- Iwasa, Y., Inoue, K. & Mizudori, M. 1980. Hydraulic Analysis of Overland Flood Flows by Means of Numerical Method. *Disaster Prevention Research Institute Annuals* 23/B-2: 305-317.
- Kuriki, M., Suetsugi, T., Umino, H., Tanaka, Y. & Kobayashi, H. 1996. Flood Simulation Manual (Proposed) – Simulation Guidelines and New Model Verification, *Public Works Research Institute, Technical Memorandum*, No.3400.
- Nakagawa, H. 1989. Research on the Evaluation of Danger Levels of Flooding and Landslides. Doctoral Thesis, Kyoto University.
- Nishihara, T. 1983. River Engineering Research on Evacuation System Based on Flood Analysis. Doctoral Thesis, Kyoto University.
- Suetsugi, T. 1995. Construction Technology Q&A, Noteworthy Points of Crisis Management During Floods. *Civil Engineering Journal* 37(3): 10-11.
- Takasao, T., Shiiba, M. & Hori, T. 1995. Modeling of Inhabitant's Attitude on Flood Disaster for Flood Refuge Simulation. *Journal of Hydroscience and Hydraulic Engineering, Japan Society of Civil Engineers* 13(1): 71-79.